

Downloaded from UvA-DARE, the institutional repository of the University of Amsterdam (UvA)
<http://hdl.handle.net/11245/2.34326>

File ID uvapub:34326
Filename 152371y.pdf
Version unknown

SOURCE (OR PART OF THE FOLLOWING SOURCE):

Type article
Title Phase-resolved spectroscopy of the low-mass X-ray binaries 1636-536/V801
Arae and 1735-444/V926 Scorpii
Author(s) T. Augusteijn, F. van der Hooft, J.A. de Jong, M.H. van Kerkwijk, J.A. van
Paradijs
Faculty FNWI: Astronomical Institute Anton Pannekoek (IAP)
Year 1998

FULL BIBLIOGRAPHIC DETAILS:

<http://hdl.handle.net/11245/1.140514>

Copyright

It is not permitted to download or to forward/distribute the text or part of it without the consent of the author(s) and/or copyright holder(s), other than for strictly personal, individual use, unless the work is under an open content licence (like Creative Commons).

Phase-resolved spectroscopy of the low-mass X-ray binaries 1636-536/V 801 Arae and 1735-444/V 926 Scorpii*

T. Augusteijn^{1,2}, F. van der Hooft², J.A. de Jong², M.H. van Kerkwijk^{2,4}, and J. van Paradijs^{2,3}

¹ European Southern Observatory, Casilla 19001, Santiago 19, Chile

² Astronomical Institute “Anton Pannekoek”, University of Amsterdam and Center for High Energy Astrophysics, Kruislaan 403, 1098 SJ Amsterdam, The Netherlands

³ Physics Department University of Huntsville in Alabama, Huntsville, AL 35899, USA

⁴ Institute of Astronomy, University of Cambridge, Madingley Road, Cambridge, CB3 0HA, UK

Received 3 October 1997 / Accepted 12 December 1997

Abstract. We present phase-resolved spectroscopy of the optical counterparts V 801 Ara and V 926 Sco of the low-mass X-ray binaries 1636-536 and 1735-444. To assist in the interpretation of the spectroscopic observations we derive new ephemerides for the photometric variations of both sources. Superior conjunction of the line emission region occurs at photometric phase ~ 0.7 in both sources, which indicates that these variations are dominated by a component originating from the point where the mass stream from the donor star intersects the outer disk. We find that the properties of 1636-536/V 801 Ara and 1735-444/V 926 Sco are very similar.

Key words: accretion, accretion disks – X-rays: stars – stars: individual: V 801 Ara – stars: individual: V 926 Sco – stars: neutron

1. Introduction

The optical continuum and line emission of luminous ($L_X \gtrsim 10^{36}$ ergs s^{-1}) low-mass X-ray binaries (LMXBs) is dominated by reprocessing of X rays in matter surrounding the X-ray source. The phasing and amplitude of orbital light-curves of LMXBs indicates that most of the optical continuum emission originates in the accretion disk around the neutron star primary, with a significant contribution from the part of the secondary that is not shielded from X rays by the disk (Van Paradijs 1983; for a review see Van Paradijs and McClintock 1995).

The optical spectra of LMXBs usually consist of a blue continuum and a few rather weak high-excitation emission lines (in particular He II 4686 Å and the N III / C III 4630 – 4650 Å

Bowen blend). Also Balmer emission lines are frequently observed. Few phase-resolved spectroscopic studies of LMXBs have been published, the main reason for this being their optical faintness, typically $V \gtrsim 17$ mag. These studies have mainly been limited to the “blue” (~ 4000 - 5000 Å) part of the spectrum; in most cases radial velocity variations were only detected in the He II 4686 Å and N III / C III 4630 – 4650 Å lines (with equivalent widths of a few Å these are usually the strongest emission lines in this spectral region), and occasionally in the hydrogen Balmer-lines (which tend to be somewhat weaker). In most objects superior conjunction of the line emission region occurs at photometric minimum, indicating that the line emission originates from the disk centered on the neutron star.

In this paper we report the results of spectroscopic observations of V 801 Ara and V 926 Sco, the optical counterparts of LMXBs 1636-536 and 1735-444, respectively. These two source are in many respects very similar; both show X-ray bursts, both are atoll sources (Hasinger and Van der Klis 1989), they have similar photometric periods (3.80 and 4.65 hr for V 801 Ara and V 926 Sco, respectively), and they are of similar apparent brightness in the optical and in X-rays (see Van Paradijs 1995 and references therein). In the past spectroscopic observations of these sources have been limited to a few low signal-to-noise spectra (see, e.g., Canizares, McClintock and Grindlay 1979; Hutchings, Cowley and Crampton 1983; Smale et al. 1984; Cowley, Hutchings and Crampton 1988) covering only a part of the orbital period. Smale and Corbet (1991) presented a phase-resolved spectroscopic study of the H α emission line in V 926 Sco. These authors found that there were two components which contributed to the radial velocity variations of H α ; a “base” component which they associate with emission from the disk centered on the neutron star primary, and a “peak” component which originates in the accretion stream or the “disk bulge” (the point where the stream intersects the outer disk).

In Sect. 2 we first present some new photometric observations of V 801 Ara and V 926 Sco, which we used to improve the photometric ephemerides and assist in the interpretation of

Send offprint requests to: T. Augusteijn

* Based on observations made at the European Southern Observatory, La Silla, Chile

Table 1. Summary of photometric observations

Source	T _{start} (HJD) -244 0000	Duration (day)	No. of obs.
1636-563/ V 801 Ara	8750.77539	0.13574	41
	8753.90527	0.04395	15
	8844.56250	0.15723	51
	9180.46777	0.24024	55
1735-444/ V 926 Sco	8826.56152	0.16602	37
	8830.60352	0.19043	60
	9195.45703	0.03711	11
	9197.47656	0.23828	34

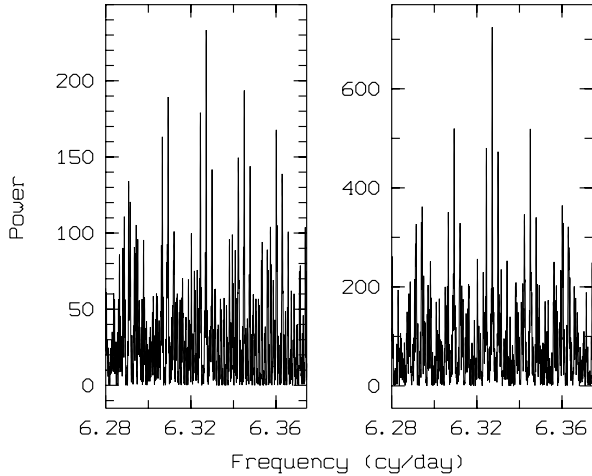


Fig. 1. Fourier spectrum of the photometric observations presented in this paper and in Van Paradijs et al. 1990 combined in the region around the period given in the literature ($P = 0.1584949$ day; frequency 6.30935 cy/day). On the right the Fourier spectrum of a sine curve with a period of 0.1580475 day sampled at the times of the observations

the spectroscopic observations. In Sect. 3 we present our spectroscopic observations. We discuss our results in Sect. 4.

2. Photometry

V 801 Ara and V 926 Sco were both observed on several occasions with a CCD camera attached to the 90cm Dutch telescope at the European Southern Observatory in Chile. A log of the observations is given in Table 1. All observations were done using a standard V filter. Typical integration times were 4 min. The observations of each source were reduced differentially with respect to several comparison stars in the field, using MIDAS and additionally written software operating in the MIDAS environment.

2.1. 1636-536/V 801 Ara

During the analysis of our spectroscopic data of V 801 Ara we obtained some puzzling results which prompted us to re-examine the period determination presented in the literature.

Table 2. Times of maximum light for 1636-536/V 801 Ara

Cycle	T _{max} (HJD) -244 0000	Error (day)	Cycle	T _{max} (HJD) -244 0000	Error (day)
0	4431.5906	0.0048	15969	6955.4360	0.0051
7	4432.6858	0.0039	16299	7007.5985	0.0031
13	4433.6320	0.0034	16312	7009.6344	0.0021
8859	5831.7150	0.0023	16318	7010.6001	0.0019
8865	5832.6806	0.0016	16324	7011.5720	0.0022
11339	6223.6754	0.0012	16330	7012.5196	0.0055
13485	6562.8386	0.0024	18066	7286.8426	0.0036
13490	6563.6336	0.0038	18078	7288.7669	0.0047
13504	6565.8310	0.0038	18084	7289.7280	0.0040
15950	6952.4270	0.0032	27922	8844.5708	0.0024
15956	6953.3949	0.0048	30048	9180.6011	0.0033

We combined our observations as listed in Table 1 with the observations presented by Van Paradijs et al. (1990). In Fig. 1 we present a Fourier spectrum using the Lomb-Scargle method (see Press and Rybicki 1989, and references therein) of all these observations in the region around the period given in the literature ($P = 0.1584949$ day; frequency 6.30935 cy/day). To remove the long term variations in the brightness of the source the data from each night were first corrected for the average brightness in that night. In Fig. 1 it can be seen that the highest peak does not correspond to the period given in the literature. The Fourier spectrum shows the typical pattern of peaks that result from the spacing of the observations, centered on the highest peak at a frequency of 6.32721 cy/day ($P = 0.1580475$ day). Also shown in Fig. 1 is the Fourier spectrum of a sine curve with a period of 0.1580475 day sampled at the times of the observations on the same frequency scale, which shows that the peak at this period in the Fourier spectrum of the observations corresponds most likely to the correct period (though there is a, in our opinion very small, possibility that the true period corresponds to the next highest peaks on either side of the highest peak which correspond to the ~ 1 cycle over 56 days aliases). We determined individual times of maximum light for each night with data covering more than 80% of the orbital period by fitting a sine curve with a period fixed to 0.158 days. In this way we obtained 22 times of maximum light which we have listed in Table 2. The errors given in this Table were derived from the individual fits assuming a good fit (i.e., the individual points were assigned errors in such a way as to obtain $\chi^2_{\text{red}} = 1.0$). The cycle counts corresponding to a period of 0.1580475 day are also listed in Table 2. From a linear least-squares fit to the arrival times we derive the following ephemeris;

$$T_{\text{max}}(\text{JD}_{\odot}) = 244\,6667.3183(26) + 0.15804738(42) \times N \quad (1)$$

$$\text{Cov}(T_0, P) = 6.7 \cdot 10^{-11} \text{ day}^2$$

where the error and covariance estimates are based on the errors in the arrival times scaled to give $\chi^2_{\text{red}} = 1.0$. From a 2nd-order polynomial fit we do not find a significant period derivative, and we derive a 3- σ lower limit to the time scale of period

Table 3. Times of maximum light for 1735-444/V 926 Sco

Cycle	$T_{\max}(\text{HJD})$ -244 0000	Error (day)
0	5904.0412	0.010
1636	6221.166	0.010
1993	6290.351	0.005
15087	8828.4090	0.0020
16986	9196.5002	0.0048

change of $|\dot{P}/P| \geq 3 \cdot 10^5 \text{ yr}$, which is consistent with period changes found in other LMXBs (see, e.g., White et al. 1995, and references therein). The scatter of the individual arrival times around the linear fit (0.014 day) is substantially greater than the typical errors in the arrival times (see Table 2) indicating a large intrinsic scatter. This is probably the result of the varying shape of the light curve (see Van Paradijs et al. 1990). We also derived ephemerides where we determined the cycle counts using periods corresponding to the two peaks on either side of the highest peak in Fig. 1 (the ~ 1 cycle over 56 days aliases; frequency 6.30935 cy/day, period 0.1584949 day and 6.34507 cy/day, 0.1576026 day, respectively). In both cases the linear fits have substantially higher scatter, and for both periods we find a significant period derivative (at the $3\text{-}\sigma$ level) on a time-scale of $|\dot{P}/P| = 3 \cdot 10^5 \text{ yr}$, which is an order of magnitude shorter than observed in any other LMXB (see White et al. 1995). Both the increased scatter and the significant period derivative are the typical product of deriving an ephemeris based on using an incorrect period, and we conclude that the ephemeris presented in Eq. (1) is the correct one. The average light curve of the data folded at the new ephemeris presented in Eq. (1) is essentially the same as the average light curve presented by Van Paradijs et al. (1990).

The reason why we derive a different period from that by Van Paradijs et al. (1990) with a relatively modest addition ($\sim 13\%$) to the data set presented in that paper is two fold: i) the statistical test given by Stellingwerf (1978) for the period search method used by the authors was shown to be incorrect (Schwarzenberg-Czerny 1989). This resulted in an overestimate of the relative significance of the different aliases which lead to the, erroneous, selection of an alias as the true period; also, ii) the distance in time between the 4 largest groups of observations used by Van Paradijs et al. (1990) are all practically an integral number of 56 days (the period derived by us is in fact the 1 cycle over 56 days alias of the period given by these authors). This has the effect that the significance of variations at the true period and its aliases are practically the same (see, e.g., Fig. 2 in Van Paradijs et al. 1990). None of the additional data presented here are at integral numbers of 56 days with respect to the rest of the data set. As can be seen in Fig. 1 this greatly reduces the strength of the power at the aliases, and allows the unambiguous identification of the true period.

2.2. 1735-444/V 926 Sco

In Table 3 we list the times of maximum light for V 926 Sco derived from our observations together with those reported in the literature (see Smale and Corbet 1991, and references therein). The arrival times for our observations of V 926 Sco were derived from a sine fit to the data with a fixed period of 0.19383 day. The fits were made to the combined data of the first two and last two observations, respectively. Using the period derived by Smale and Corbet we are able to maintain the cycle count over the whole data set, and the corresponding cycles are listed in Table 3. From a linear least-squares fit we derive the following ephemeris;

$$T_{\max}(\text{JD}_{\odot}) = 244\,7288.0143(25) + 0.19383351(32) \times N \quad (2)$$

$$\text{Cov}(T_0, P) = 6.1 \cdot 10^{-10} \text{ day}^2$$

with a $\chi^2_{\text{red}} = 0.53$ for 3 degrees of freedom. We do not find any significant period derivative, and we derive a $3\text{-}\sigma$ lower limit to the time-scale of period change of $|\dot{P}/P| \geq 1 \cdot 10^6 \text{ yr}$.

The phasing as derived from the ephemerides presented in Eqs. (1) and (2) will be used throughout the remainder of this paper.

3. Spectroscopy

V 801 Ara and V 926 Sco were observed during two consecutive nights in 1989 with the ESO-3.6m telescope, using the ESO Faint Object Spectrograph (EFOSC) and a grism (B150) which covers the wavelength range 3600-5500 Å at 1.8 Å/pixel. The data were recorded with an RCA 1024×640 CCD and binned with a factor two in both the spatial and dispersion direction in order to reduce the readout noise. The slit width was adapted to the seeing, and we used a 1''5 slit during the first night and a 2'' slit during the second night.

We observed V 801 Ara on July 5th from UT 00:49 to 07:50, collecting 13 spectra with an integration time of 30 min (20 min for the first 2 spectra). Monitoring of V 926 Sco started the next night at UT 00:36 and lasted until UT 9:05. We obtained 15 spectra of this source with an integration time of 30 min each. Wavelength calibration spectra using an He-Ar lamp were obtained every 4 spectra, and at the beginning and end of the observations. After each calibration spectrum the target was recentered in the slit. The resolution as derived from the FWHM of these He-Ar calibration spectra was 7.5 and 9.5 Å for the first and second night, respectively.

All CCD frames were corrected for the bias and flat fielded in the standard way. All stellar spectra were extracted from the CCD frames using an optimal extraction algorithm similar to that of Horne (1986) and wavelength calibrated using the time-nearest He-Ar exposure. During both nights additional spectra of flux standards were obtained. The spectra of V 801 Ara were flux calibrated using LDS 749B (Oke 1974), and for the flux calibration of the spectra of V 926 Sco the standard L870-2 (Oke 1974) was used.

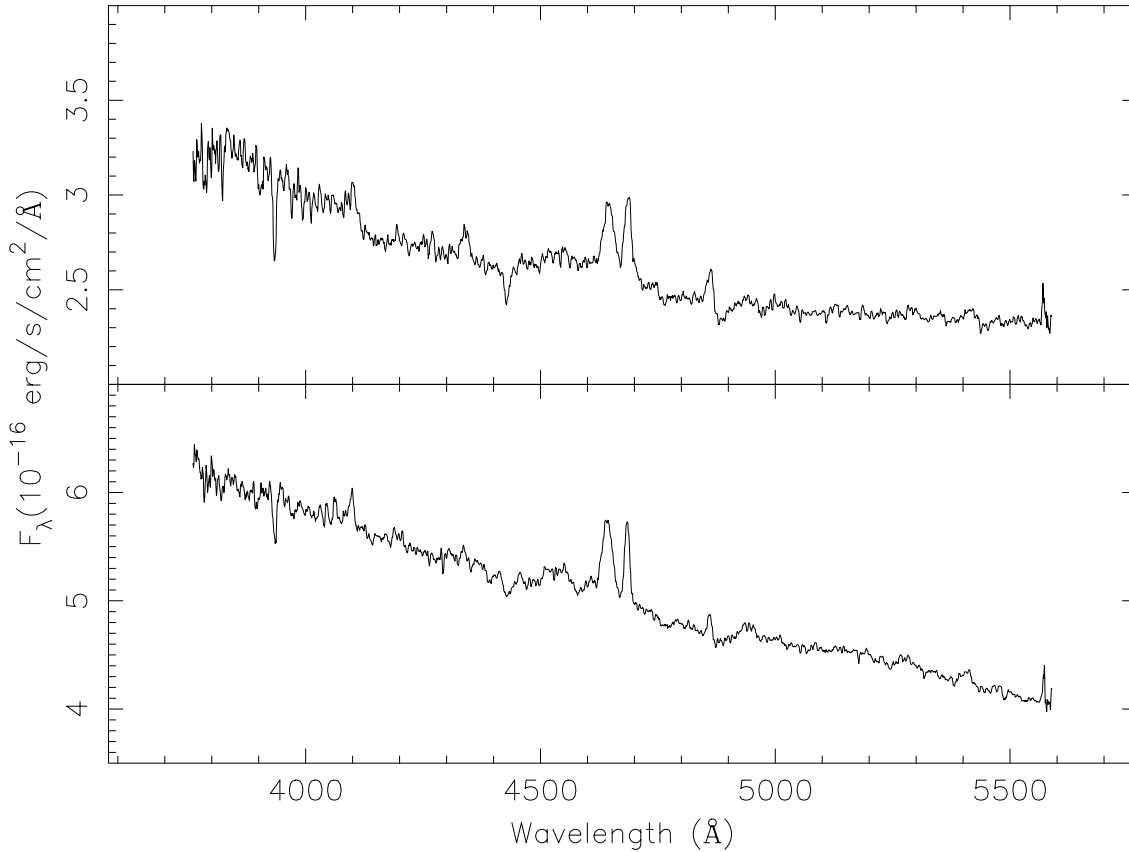


Fig. 2. Average spectrum of 1636-536/V 801 Ara (top), and 1735-444/V 926 Sco (bottom)

3.1. Average spectrum

The average spectra of V 801 Ara and V 926 Sco are presented in Fig. 2. Both spectra are typical for LMXBs, showing prominent emission lines of He II 4686 Å and N III/C III 4630–4650 Å superposed on a blue continuum. The N III/C III blend is primarily due to three N III 4634–4642 Å emission lines which result from the Bowen process (Bowen 1935), as was proposed by McClintock et al. (1975). The relatively strong emission at ~ 4100 Å in the spectrum of V 926 Sco might be (partly) due to the N III doublet, since no significant H δ emission is expected when H γ is nearly absent (McClintock et al. 1978). In both sources the ratio in strength of the Balmer lines to the N III/C III 4630–4650 Å and He II 4686 Å emission is reversed with respect to Sco X-1 (see, e.g., Schachter et al. 1989). In both sources the He II and N III/C III emission lines are superposed on a broad emission “hump” which extends approximately from 4500 to 4700 Å. A similar hump is also present in the spectrum of Sco X-1, and Schachter et al. (1989) suggested that it is caused by a blend of Fe II emission lines. In both spectra there is some evidence for the presence of He II emission of the Pickering series He II 5412 Å (Pi γ) and He II 4200 Å (Pi11); the latter might be blended with N III/C III 4195, 4200, 4215 Å emission lines. Interstellar absorption lines of Ca II 3934 Å and the diffuse bands at 4430 Å and 4880 Å are also present in both

Table 4. Equivalent widths (EWs) of identified emission and absorption lines in the average spectra of V 801 Ara and V 926 Sco

Line	$\lambda(\text{Å})$	EW(Å) ^a	
		V 801 Ara	V 926 Sco
Ca II	3934	1.1(2)	0.5(1)
H δ	4102	−0.6(2)	−0.5(1)
H γ	4341	−0.8(1)	−0.2(1)
Diff. IS	4430	1.2(1)	0.7(2)
N III/C III	4630-4650	−3.1(3)	−3.2(2)
He II	4686	−2.7(3)	−1.7(1)
H β	4861	−0.9(2)	−0.5(1)
Diff. IS	4880	1.2(2)	0.4(1)
He II	5412	−0.5(1)	−0.6(1)

^a Negative values indicate emission

averaged spectra. The identified lines in both spectra and their equivalent widths (EWs) are listed in Table 4. In this table negative values refer to emission lines. The errors in the equivalent widths were estimated by looking at the scatter in the values when selecting different wavelength intervals to define the local continuum.

3.2. Radial-velocity variations

Attempts to fit the individual N III Bowen lines in the N III/C III 4630 – 4650 Å blend in the averaged spectra with a multiple Gaussian profile were not successful and we decided to fit this blend with one Gaussian profile. Furthermore, the N III/C III blend and the He II emission lines are not well separated (see Fig. 2) and we, therefore, fitted the He II and N III/C III emission lines simultaneously with 2 Gaussians. In order to constrain the fit better we also fitted these lines together, using two Gaussian profiles, with their separation fixed to the literature value; the rest wavelength of the N III/C III blend (4645.3 Å) has been calculated as the average of the wavelengths of the 6 individual components, weighted by the laboratory intensities as given by McClintock et al. (1975).

In this way we have derived for each spectrum three radial velocity measurements, one from the combined fit to the He II and N III/C III emission lines, and one for each of the emission lines separately. The results are listed in Table 5. The errors in the velocities are the formal errors derived from the fit.

To check the accuracy of our wavelength calibration we measured the Ca II interstellar absorption line in the individual spectra. For V 801 Ara we derived an average velocity of +1 km/s with a standard deviation of 73 km/s. This latter value compares reasonably well to the formal error of the individual fits to the Ca II lines which are typically ~ 40 km/s.

In Fig. 3 (top) we present the radial velocities derived for the combined fit to the He II and N III/C III lines in the spectra of V 801 Ara folded at the ephemeris given in Eq. (1). The radial-velocity variations for the fits to the He II line and the N III/C III blend separately look very similar to the curve presented in Fig. 3, where we note that the curve of the combined fit most resembles the radial-velocity variations of the He II line alone (see also Table 5). This is expected as the He II line is much narrower than the N III/C III blend, and this line will therefore dominate the variations obtained from the combined fit. The system velocity and the radial velocity amplitude were derived from a least-squares sine fit to the velocities listed in Table 5. The results for the velocities from the combined fit, and from the fit to the He II and N III/C III lines separately are listed in Table 6, and the corresponding fit for the velocities from the combined fit to the He II and N III/C III lines is shown in Fig. 3.

For V 926 Sco the Ca II absorption line is too weak to be fitted in the individual spectra of this source. We, therefore, averaged the spectra taken in between He-Ar calibration spectra (see above). In this we we derive velocities of +127(23), +92(26), -68(25) and +91(61) km/s, where the first three values are derived from the average of 4 spectra, and the last value from the average of 3 spectra. The values in parenthesis are the formal errors derived from the fit. It is clear that the velocity derived from the average of the third group of spectra is significantly different from the other values. A simple explanation might be that the source was not properly recentered in the slit after the wavelength calibration spectrum taken immediately before the third set of 4 spectra, or moved out of the slit (either by movement of the telescope or due to atmospheric diffraction) in the

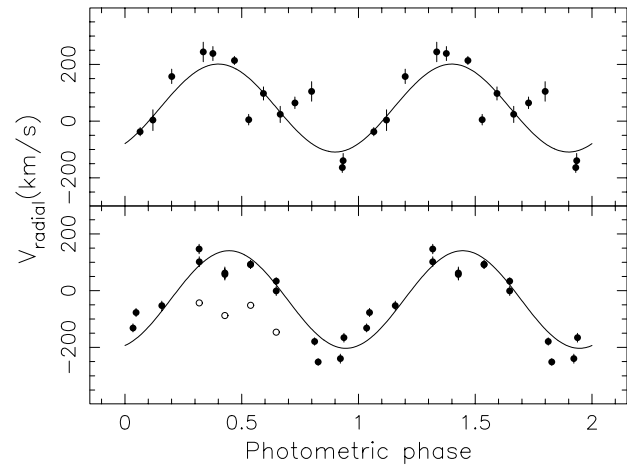


Fig. 3. Radial-velocity variations of the combined fit to the He II + N III/C III lines for 1636-536/V 801 Ara (top), and 1735-444/V 926 Sco (bottom) folded at their respective photometric periods presented in Eqs. (1) and (2). The drawn lines represent the sine fits to these variations (see Table 6). For 1735-444/V 926 Sco (bottom panel) we also show as open circles the uncorrected velocities of the 4 spectra that were shifted (see text)

course of the observation. However, all the observation were done using an autoguider, the affected observation were made at relatively low (1.14-1.40) airmass, and the total counts in the spectra do not show any trend with time. As the velocities determined from the average spectra for the remaining three groups of observations do not differ significantly we have decided to correct the spectra in the third group. This was done by shifting the discrepant spectra in wavelength by 2.26 Å, which correspond to the difference in velocity of 172 km/s (at $\lambda = 3934$ Å) between the third group of observations and the average of the remaining three groups of observations (see above).

In the bottom part of Fig. 3 we present the radial velocities derived for the combined fit to the He II and N III/C III lines in the spectra of V 926 Sco folded at the ephemeris given in Eq. (2). The system velocity and the radial velocity amplitude were derived from a least-squares sine fit to the velocities listed in Table 5. The results are given in Table 6, and the corresponding fit for the velocities from the combined fit to the He II and N III/C III lines is shown in Fig. 3. Also for V 926 Sco the radial-velocity curve obtained from the combined fit to the He II and N III/C III lines is dominated by the He II line (see Tables 5 and 6). In Fig. 3 we also show the 4 uncorrected velocities as open circles. We note that fits to the velocities excluding the corrected velocities gives very similar results to the fits using all velocities including the corrected points, which supports our decision to shift these points.

The results we derived for V 926 Sco are fairly similar to the results obtained by Smale and Corbet (1991) for the H α emission line. These authors found radial-velocity variations with two components. One component that dominates in the line wings (or “base”) of the line, has a low velocity amplitude, and superior conjunction for this component occurs at phase

Table 5. Radial velocities of V 801 Ara and V 926 Sco

Source	HJD −244 7700	V ^a (km/s)	V(km/s)	V(km/s)	EW(Å)
		He II + N III / C III	He II	N III / C III	He II + N III / C III
1636-536/ V 801 Ara	12.54516	238(25)	240(43)	216(44)	−7.8
	12.55973	214(14)	216(39)	171(39)	−6.9
	12.57937	97(23)	70(48)	225(48)	−7.3
	12.60069	64(20)	9(25)	80(25)	−5.2
	12.63272	−164(18)	−165(41)	−174(41)	−7.4
	12.65403	−37(15)	−17(29)	−122(30)	−5.0
	12.67535	158(25)	227(40)	−35(41)	−5.1
	12.69666	244(34)	242(54)	−104(54)	−6.9
	12.72742	5(19)	−16(39)	90(40)	−6.1
	12.74874	24(29)	−18(38)	48(38)	−5.4
	12.77005	105(34)	43(51)	232(52)	−7.0
	12.79135	−139(25)	−124(51)	−197(52)	−6.2
	12.82069	3(37)	2(77)	−7(77)	−5.4
1735-444 V 926 Sco	13.54047	147(17)	157(19)	96(35)	−5.3
	13.56178	63(21)	84(23)	−25(40)	−5.0
	13.58309	91(13)	99(15)	48(28)	−5.8
	13.60441	33(12)	56(12)	−149(29)	−5.7
	13.63923	−251(12)	−251(13)	−268(25)	−5.1
	13.66064	−166(16)	−141(18)	−251(30)	−4.4
	13.68195	−77(14)	−54(15)	−193(32)	−5.0
	13.70326	−53(16)	−12(17)	−207(31)	−4.8
	13.73436 ^b	102(17)	185(17)	−112(24)	−4.7
	13.75566 ^b	58(20)	74(24)	18(31)	−5.0
	13.77698 ^b	94(14)	117(15)	−1(28)	−5.0
	13.79829 ^b	−1(16)	19(20)	−49(26)	−5.1
	13.83016	−179(13)	−170(15)	−222(26)	−4.9
	13.85147	−240(16)	−226(19)	−291(30)	−6.4
	13.87324	−131(14)	−121(16)	−186(31)	−4.5

^a Separation of Gaussians fixed to literature value (see text)

^b Velocities corrected using the Ca II absorption line (see text)

Table 6. System parameters

line(s)	ϕ^a	K (km/s)	γ (km/s)
1636-536/V 801 Ara			
He II & N III / C III ^b	0.650(39)	155(32)	46(22)
He II	0.618(35)	154(33)	59(22)
N III / C III	0.789(45)	149(36)	18(27)
1735-444/V 926 Sco			
He II & N III / C III ^b	0.696(27)	172(17)	−31(13)
He II	0.648(22)	184(20)	−6(14)
N III / C III	0.656(21)	140(20)	−127(15)

^a Phase of superior conjunction with respect to Eqs. (1) and (2). Phase zero corresponds to photometric maximum

^b Separation of Gaussians fixed to literature value (see text)

0.43(3) as calculated with respect to the ephemeris presented in Eq. (2). The second component dominates the line center (or “peak”) of the line, has a high velocity amplitude and superior conjunction occurs at phase 0.77(2). If the photometric variations are the result of the varying aspect of the heated side of the

secondary these two components are naturally identified with emission originating from the disk centered on the neutron star (the “base” component) and from the bulge (the “peak” component). The phasing of the lines presented here for V 926 Sco in Table 6 agree somewhat better with the phasing derived by Smale and Corbet (1991) from fits to the whole H α line profile (phase 0.70(2)), while the amplitude is somewhat smaller than these authors derived for the “peak” component. This indicates that both the “peak” and “base” components contribute to the radial velocity variations we derive from the the He II and N III / C III lines. Unfortunately, the resolution of our spectra is insufficient to separate the contribution from the disk and the bulge, but a significant amount of emission must arise from the bulge to explain the observed radial-velocity variations. Smale and Corbet (1991) found that the bulge in V 926 Sco contributes about 20% to the H α emission.

The phasing and amplitudes of the emission lines with respect to the photometric variations for V 801 Ara presented in Table 6 are very similar to those derived for V 926 Sco. It, therefore, seems reasonable to assume that a similar explanation in terms of radial velocity variations dominated by emission from the bulge, but with a significant contribution from emission orig-

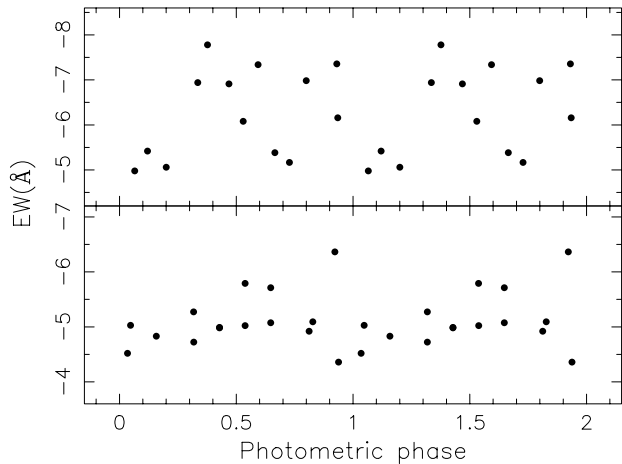


Fig. 4. The equivalent width of the He II and N III/C III lines combined for 1636-536/V 801 Ara (top), and 1735-444/V 926 Sco (bottom) folded at their respective photometric periods presented in Eqs. (1) and (2)

inating from the disk centered on the neutron star, is also valid for V 801 Ara. One might expect that also the equivalent widths (EWs) of the He II and N III/C III lines show a variation with phase. We found that it was very difficult to determine the continuum in between the He II and N III/C III line accurately. We, therefore, decided to determine the EWs of these lines together and we list the results in Table 5 (one might notice that the average of these values are slightly higher than the combined EWs of He II and N III/C III listed in Table 4, which is the result of the different way in which we determined the continuum level). In Fig. 4 we present the EWs listed in Table 5 for V 801 Ara and V 926 Sco as function of phase with respect to Eqs. (1) and (2), respectively. It can be seen that for both sources there is no indication for any variations as function of phase.

The system velocity derived for the N III/C III blend in V 926 Sco seems to be different from that of the He II line. This may be the result of our particular choice for the rest wavelength for the N III/C III blend (see above), but it is not clear why we do not find a similar difference in V 801 Ara. The value of the system velocity for V 926 Sco is very different from that obtained by Smale and Corbet for the H α emission line. However, given the problems we had with the wavelength calibration of some of the spectra of V 926 Sco (see above) we do not consider the system velocities derived for either source to be very reliable, and we will not consider them in the remainder of this paper. For the same reason we also ignored the heliocentric velocity correction which is -8 km/s for both sources.

4. Discussion

4.1. Emission from the bulge

Detailed models show that the He II 4686 Å and (of course) the Bowen N III/C III 4630 – 4650 Å emission from LMXBs is caused by reprocessing of X-rays, predominantly in the outer

disk (see, e.g., Raymond 1992). The phasing of the radial velocity curves of both sources indicate that the velocity variations contains a significant component originating in the bulge. This indicates that the distribution of X-ray reprocessing is not axisymmetric, and that the disk bulge subtends a rather large solid angle as seen from the X-ray source. Evidence for large bulges in disks of LMXBs has been inferred from optical and X-ray light curve analysis of 1822-371 (Hellier and Mason 1989) and from the presence of X-ray dips – but not eclipses – in 1254-690 (Courvoisier et al. 1986) and 1755-338 (White et al. 1984). It is generally believed that the photometric variations observed in LMXBs are the result of the varying aspect of the heated face of the companion (see, e.g., Van Paradijs and McClintock 1995). However, a large bulge is also expected to contributed significantly to the optical continuum emission. Motch et al. (1987) estimated that in the dipping source 1254-690 the hot spot can contribute up to 30% of the light emitted by the disk. Such a contribution is comparable to the contribution from the heated face of the secondary, and could have a significant effect on the observed orbital light curve. A variable contribution from the bulge to the optical light curve might explain the variable shape of the optical light curve of V 801 Ara (see Van Paradijs et al. 1990, their Fig. 1), and the large scatter in the arrival times of maximum light (see Sect. 2.1).

V 801 Ara and V 926 Sco are not the only LMXBs that show emission line variations that point to a strong component originating in the bulge. Other sources were evidence is found for such a component are 0748-676 (Crampton et al. 1986), 1822-371 (Cowley et al. 1982a, Mason et al. 1982) and 2129+470 in its high state (Thorstensen and Charles 1982, Horne et al. 1986). It occurs to us that all these sources have relatively short orbital periods (~ 4 -5 hrs), but that in LMXBs with longer orbital periods ($\gtrsim 1$ day) such a strong component is not observed, and the radial-velocity variations are dominated by a component coming from a region in the disk centered on the primary (0921-630: Cowley et al. 1982b, Branduardi-Raymont et al. 1983; Sco X-1: Crampton et al. 1976, LaSala and Thorstensen 1985; Her X-1: Crampton and Hutchings 1974). Cyg X-2 is somewhat exceptional in that the radial velocity variations of the He II 4686 Å emission line varies in phase with the absorption lines from the giant secondary, indicating an origin on the heated phase of the secondary (Cowley et al. 1979). A possible explanation for the absence of a significant emission line component from the bulge in sources with long period is that the bulge is relatively small. The size of the accretion disk, and the height of the disk rim in these sources is expected to be larger. Furthermore, compared to sources with short orbital periods the accretion stream will have fallen less deep into the potential well of the neutron star primary when it hits the accretion disk and forms the bulge. It, therefore, also seems likely that the vertical extend of the bulge is smaller in sources with long orbital periods, and that the solid angle of the bulge as seen by the central X-ray source is smaller.

4.2. A comparison of the two sources

Following Van Paradijs and McClintock 1994, one can estimate the distance to 1636-536/V 801 Ara and 1735-444/V 926 Sco from the peak flux observed during type I X-ray bursts that show radius expansion. Using the values listed by Damen et al. (1990; their Table 2) we derive distances of 5.9 and 9.1 kpc for 1636-536/V 801 Ara and 1735-444/V 926 Sco, respectively. The corresponding persistent X-ray flux (2-10 keV) for these sources (see Van Paradijs 1994) are $1.7 \cdot 10^{37}$ and $3.1 \cdot 10^{37}$ erg/s, respectively.

From the strength of the diffuse interstellar absorption band at 4430 Å (see Table 4) we can estimate the reddening towards the sources. Using the relation given by Tüg and Schmidt-Kaler (1981) we derive $E(B - V) = 0.45$ and 0.24 mag for 1636-536/V 801 Ara and 1735-444/V 926 Sco, respectively. These values are in good agreement with the values found by Van Paradijs et al. (1986), who derived from observation of early type stars that the extinction in the direction of 1636-536/V 801 Ara remains approximately constant at 0.4 mag for distances greater than 2 kpc; for 1735-444/V 926 Sco they found for distances greater than 2 kpc an average reddening of 0.14 ± 0.07 mag. The result for 1636-536/V 801 Ara is in disagreement with the result of Lawrence et al (1983) who determined a reddening of 0.8 mag from the analysis of a multicolour observation from this source.

Assuming $A_V = 3.1 E(B - V)$, and the distances derived above we obtain for the absolute visual brightness of the systems $M_V = 2.3$ and 2.0 for 1636-536/V 801 Ara and 1735-444/V 926 Sco, respectively. Given that the intrinsic luminosity in X-rays of the two sources is very similar, the absolute visual brightness of the systems are consistent with the idea that the optical luminosity of LMXBs is dominated by reprocessing of X-rays in material surrounding the X-ray source.

From the fact that the radial velocity amplitudes of V 801 Ara and V 926 Sco are similar (see Table 6) and seem to have the same origin, and given the fact that the amplitude of the photometric light curve (~ 0.2 mag, see Van Amerongen et al. 1987 and Van Paradijs et al. 1990) are practically the same, it seems that the inclination angle of 1636-536/V 801 Ara and 1735-444/V 926 Sco are also similar.

Acknowledgements. TA acknowledges support by the Netherlands Foundation for Research in Astronomy (NFRA) with financial aid from the Netherlands Organization for Scientific Research (NWO) under contract number 782-371-038. We gratefully acknowledge the referee (Manfred Pakull) for his valuable comments.

References

Branduardi-Raymont, G., Corbet, R.H.D., Mason, K.O., et al. 1983, MNRAS, 205, 403
 Canizares, C.R., McClintock, J.E., Grindlay, J.E. 1979, ApJ, 234, 556
 Courvoisier, T.J.-L., Parmar, A.N., Peacock, A., Pakull, M.W. 1986, ApJ, 309, 265
 Cowley, A.P., Crampton, D., Hutchings, J.B. 1979, ApJ, 231, 539
 Cowley, A.P., Crampton, D., Hutchings, J.B. 1982, ApJ, 255, 596
 Cowley, A.P., Crampton, D., Hutchings, J.B. 1982, ApJ, 256, 605

Cowley, A.P., Hutchings, J.B., Crampton, D. 1988, ApJ, 333, 906
 Crampton, D., Hutchings, J.B. 1974, ApJ, 191, 483
 Crampton, D., Cowley, A.P., Hutchings, J.B., Kaat, C. 1976, ApJ, 207, 907
 Crampton, D., Cowley, A.P., Stauffer, J., Ianna, P., Hutchings, J.B. 1986, ApJ, 306, 599
 Damen, E., Magnier, E., Lewin, W.H.G., et al. 1990, A&A, 237, 103
 Hasinger, G., Van der Klis, M. 1989, A&A, 225, 79
 Hellier, C., Mason, K.O. 1989, MNRAS, 239, 715
 Hellier, C., Mason, K.O., Smale, A.P., Kilkenny, D. 1990, MNRAS 244, 39p
 Horne, K., 1986, PASP, 98, 609
 Horne, K., et al. 1986, MNRAS, 218, 63
 LaSala, J., Thorstensen, J.R. 1985, AJ, 90, 2077
 Mason, K.O., Murdin, P.G., Tuohy, I.R., Seitzer, P., Branduardi-Raymont, G. 1982, MNRAS, 200, 793
 Hutchings, J.B., Cowley, A.P., Crampton, D. 1983, PASP, 95, 23
 Lawrence, A. Cominsky, L., Engelke, C., et al. 1983, ApJ, 271, 793
 McClintock, J.E., Canizares, C.R., Tarter, C.B. 1975, ApJ, 198, 641
 McClintock, J.E., Canizares, C.R., Backman, D.E. 1978, ApJ, 223, L75
 Motch, C., Pedersen, H., Beuermann, K., Pakull, M.W., Courvoisier, T.J.-L. 1987, ApJ, 313, 792
 Oke, J. B. 1974, ApJS, 27, 21
 Patterson, J. 1984, ApJS, 54, 443
 Press, W.H., Rybicki, G.B. 1989, ApJ, 338, 277
 Raymond, J.C. 1992, ApJ 412, 267
 Schachter, J., Filippenko, A.V., Kahn, S.M. 1989, ApJ, 340, 1049
 Schwarzenberg-Czerny, A. 1989, MNRAS 241, 153
 Smale, A.P., Charles, P.A., Tuohy, I.R., Thorstensen, J.R. 1984, MNRAS, 207, 29p
 Smale, A.P., Corbet, R.H.D. 1991, ApJ, 383, 853
 Stellingwerf, R.F. 1978, ApJ 224, 953
 Thorstensen, J.R., Charles, P.A. 1982, ApJ, 253, 756
 Tüg, H., Schmidt-Kaler, Th. 1981, A&A, 94, 16
 Van Amerongen, S.F., et al. 1987, A&A, 185, 147
 Van Paradijs, J. 1983, in: Accretion Driven Stellar X-ray Sources, eds. W. H. G. Lewin & E. P. J. Van den Heuvel (Cambridge University Press), p. 189
 Van Paradijs, J., Van Amerongen, S.F., Damen, E., Van der Woerd, H. 1986, A&AS, 63, 71
 Van Paradijs, J., Van der Klis, M., Van Amerongen, S.F., et al. 1990, A&A, 234, 181
 Van Paradijs, J. 1991, in: Neutron stars: Theory and Observation, eds. J. Ventura & D. Pines (Dordrecht: Kluwer Academic Press), p. 245
 Van Paradijs, J. 1995, in: X-ray Binaries, eds. W.H.G. Lewin, J. Van Paradijs, & E.P.J. Van den Heuvel (Cambridge: Cambridge University Press), p. 536
 Van Paradijs, J. & McClintock, J. E. 1994, A&A, 290, 133
 Van Paradijs, J. & McClintock, J. E. 1995, in: X-ray Binaries, eds. W. H. G. Lewin, J. Van Paradijs, & E. P. J. Van den Heuvel (Cambridge: Cambridge University Press), p. 58
 White, N.E., et al. 1984, ApJ, 283, L9
 White, N.E., Nagase, F., Parmar, A.N. 1995, in: X-ray Binaries, eds. W. H. G. Lewin, J. Van Paradijs, & E. P. J. Van den Heuvel (Cambridge: Cambridge University Press), p. 1